Analytical representation of a black hole puncture solution

Thomas W. Baumgarte* and Stephen G. Naculich
Department of Physics and Astronomy, Bowdoin College, Brunswick, Maine 04011, USA
(Received 8 January 2007; published 13 March 2007)

The ''moving-puncture'' technique has led to dramatic advancements in the numerical simulations of binary black holes. Hannam *et al.* have recently demonstrated that, for suitable gauge conditions commonly employed in moving-puncture simulations, the evolution of a single black hole leads to a well-known, time-independent, maximal slicing of Schwarzschild spacetime. They construct the corresponding solution in isotropic coordinates numerically and demonstrate its usefulness, for example, for testing and calibrating numerical codes that employ moving-puncture techniques. In this brief report we point out that this solution can also be constructed analytically, making it even more useful as a test case for numerical codes.

DOI: 10.1103/PhysRevD.75.067502 PACS numbers: 04.20.Jb, 04.25.Dm, 04.20.Ex

Numerical relativity simulations of binary black holes have recently achieved a remarkable breakthrough. Since Pretorius's initial announcement of a successful simulation of binary black hole coalescence and merger [1], several groups have reported similar success (e.g. [2–8]). Of these, Refs. [1,6] adopt a ''generalized harmonic'' formulation of general relativity [9,10] and eliminate the black hole singularity from the numerical grid with the help of ''black hole excision.'' All the other groups adopt the BSSN formulation of the ADM equations [11,12] together with a ''moving-puncture'' method to handle singularities.

The idea of the original puncture method was to factor out from the spatial metric (or more specifically from the conformal factor) an analytic term that represents the singular terms at a black hole singularity, and treat only the remaining regular terms numerically. This approach was very successful for the construction of initial data (e.g. [13]), but did not achieve long-term stable evolutions in dynamical simulations (e.g. [14,15]). The problem may be associated with the need for a coordinate system that leaves the puncture—and hence the black hole singularity—at a prescribed location in the numerical grid, given by the singularity in the analytical function. The breakthrough in the recent dynamical puncture simulations is based on the idea of using a ''moving'' puncture in which no singular term is factored out. Care is taken that the singularity never hits a grid point in the numerical grid, but otherwise the puncture is allowed to move around freely. With a set of suitable coordinate conditions, found empirically, this prescription leads to remarkably stable evolutions. Clearly, this raises the question of how it can be that the presence of singularities does not spoil the numerical calculation. This issue has been clarified recently by Hannam *et al.* [16,17].

For a single black hole, a moving-puncture simulation starts out with a slice of constant Schwarzschild time expressed in isotropic coordinates. These coordinates do not penetrate the black hole interior, and instead cover two copies of the black hole exterior, corresponding to two sheets of asymptotically flat ''universes,'' connected by an Einstein-Rosen bridge at the black hole horizon. The singularity at isotropic radius $r = 0$, where the conformal factor $\psi = 1 + M/(2r)$ diverges with $1/r$, corresponds to the asymptotically flat end of the ''other'' universe, and is therefore a coordinate singularity only.

Typically, moving-puncture simulations use some variant of the ''1 + log'' slicing condition [18]

$$(\partial_t - \beta^i \partial_i)\alpha = -2\alpha K \tag{1}$$

as well as a ''$\tilde{\Gamma}$-freezing'' condition [19]. In [16] the authors show that, with these coordinate conditions, the evolution quickly settles down into a new time-independent solution that is different from the initial data. In this new time-independent solution the conformal factor features a $1/\sqrt{r}$ singularity at $r = 0$ instead of a $1/r$ singularity, meaning that the slice has disconnected from the other asymptotically flat end, and instead terminates on a surface of finite Schwarzschild coordinate radius. For the slicing condition (1), Ref. [16] found this limiting surface to be at a Schwarzschild (or areal) radius of $R = 1.3M$. The numerical grid therefore does not include the spacetime singularity at $R = 0$. Instead, the singularity at $r = 0$ is again only a coordinate singularity, which helps to explain the success of this numerical method.

In [17] (hereafter HHBGSO) the authors consider the alternative slicing condition

$$\partial_t \alpha = -2\alpha K. \tag{2}$$

Dynamical evolutions again settle down quickly into a new time-independent solution, which in this case has to be a maximal slice (with $K = 0$) of Schwarzschild spacetime. A family of time-independent, maximal slicings of the Schwarzschild spacetime is given by the expressions [20] for the spatial metric,

$$\gamma_{ij} dx^i dx^j = f^{-2} dR^2 + R^2 d^2\Omega, \tag{3a}$$

*Also at Department of Physics, University of Illinois, Urbana, Il 61801, USA.

the lapse,

$$\alpha = f, \tag{3b}$$

and the shift vector,

$$\beta^R = \frac{Cf}{R^2}. \tag{3c}$$

Here we assume spherical polar coordinates, and the function f,

$$f = \left(1 - \frac{2M}{R} + \frac{C^2}{R^4}\right)^{1/2}, \tag{3d}$$

depends on both the areal radius R and an arbitrary parameter C. For $C = 0$ we recover Schwarzschild coordinates. HHBGSO provide evidence that the dynamical evolution, starting from a slice of constant Schwarzschild time and using the slicing condition (2), settles down to a member of the family (3) with $C = 3\sqrt{3}M^2/4$, which has a limiting surface at $R = 3M/2$. For numerical purposes it is desirable to obtain this solution in isotropic coordinates. HHBGSO construct this solution numerically, and then proceed to show that the solution is indeed time independent. This solution provides a very powerful test for numerical codes that use the moving-puncture method. Using this solution as initial data, the time evolution should lead to a time-independent solution, so that any deviation from the initial data is a measure of the numerical error.

In this brief report we point out that this solution in isotropic coordinates can be constructed analytically, making it an even more useful tool for code testing.

To transform the solution (3) into isotropic coordinates, we identify the spatial metric (3a) with its counterpart in isotropic coordinates,

$$f^{-2}dR^2 + R^2 d^2\Omega = \psi^4(dr^2 + r^2 d^2\Omega), \tag{4}$$

where ψ is the conformal factor and r the new isotropic radius. From this identification we have

$$R^2 = \psi^4 r^2 \tag{5}$$

and

$$f^{-2}dR^2 = \psi^4 dr^2, \tag{6}$$

which we can combine to find

$$\pm \int \frac{dr}{r} = \int \frac{1}{f}\frac{dR}{R} = \int \frac{RdR}{\sqrt{R^4 - 2MR^3 + C^2}}. \tag{7}$$

In the general case, the right-hand side may be expressed in terms of elliptic integrals of the first and third kinds, which of course cannot be written in terms of elementary functions. The integral simplifies, however, when two or more roots of the quartic equation $R^4 - 2MR^3 + C^2 = 0$ coincide, which occurs precisely when the discriminant

$$16C^4(16C^2 - 27M^4) \tag{8}$$

vanishes (see, e.g., [21]). This happens for two different values of C^2. In the case $C = 0$, integration of (7) yields the familiar isotropic form of the Schwarzschild metric.

Remarkably, the discriminant also vanishes for $C = 3\sqrt{3}M^2/4$, the case of particular interest here. In this case, the quartic polynomial has a double root at $R = 3M/2$, and the integral can be written

$$\pm \int \frac{dr}{r} = \int \frac{RdR}{(R - 3M/2)\sqrt{R^2 + RM + 3M^2/4}}, \tag{9}$$

which yields

$$\begin{aligned}\pm \ln r = {} & \frac{1}{\sqrt{2}} \ln\left[\frac{2R - 3M}{8R + 6M + 3(8R^2 + 8MR + 6M^2)^{1/2}}\right] \\ & + \ln[2R + M + (4R^2 + 4MR + 3M^2)^{1/2}] \\ & + \text{const.}\end{aligned} \tag{10}$$

For the positive sign, we then have

$$\begin{aligned} r &= \left[\frac{2R + M + (4R^2 + 4MR + 3M^2)^{1/2}}{4}\right] \\ &\quad \times \left[\frac{(4 + 3\sqrt{2})(2R - 3M)}{8R + 6M + 3(8R^2 + 8MR + 6M^2)^{1/2}}\right]^{1/\sqrt{2}} \\ &= R\left[1 - \frac{M}{R} - \frac{M^2}{2R^2} + \cdots\right] \end{aligned} \tag{11}$$

where we fixed the constant of integration by requiring that $r \to R$ as $R \to \infty$. Equation (11) gives the value of the isotropic radius r as a function of the areal radius R. As expected, we find $r \to 0$ in the limiting case $R \to 3M/2$.

From Eqs. (5) and (11), we obtain the conformal factor

$$\begin{aligned}\psi = {} & \left[\frac{4R}{2R + M + (4R^2 + 4MR + 3M^2)^{1/2}}\right]^{1/2} \\ & \times \left[\frac{8R + 6M + 3(8R^2 + 8MR + 6M^2)^{1/2}}{(4 + 3\sqrt{2})(2R - 3M)}\right]^{1/2\sqrt{2}}.\end{aligned} \tag{12}$$

Although Eq. (11) cannot be inverted to yield R as a function of r, Eqs. (11) and (12) may be used parametrically to make a plot of ψ vs r (see Fig. 1). Figure 1 also includes the asymptotic limits

$$\psi \to \begin{cases} \left(\frac{3M}{2r}\right)^{1/2} & r \to 0, \\ 1 + \frac{M}{2r} & r \to \infty. \end{cases} \tag{13}$$

The lapse

$$\alpha = \left(1 - \frac{2M}{R} + \frac{27M^4}{16R^4}\right)^{1/2} \tag{14}$$

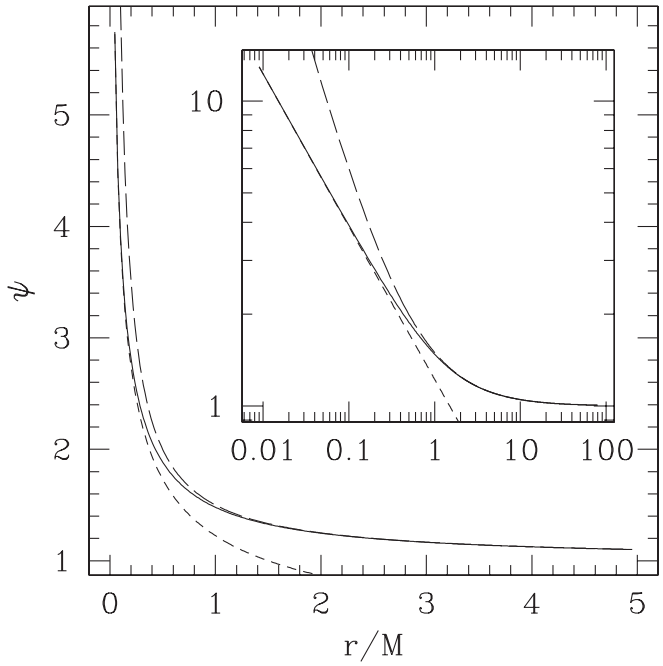

FIG. 1. The conformal factor ψ as a function of isotropic radius r (solid line). The short-dashed line shows the asymptotic value $\psi = \sqrt{3M/(2r)}$ in the limit $r \to 0$; the long-dashed line shows the asymptotic value $\psi = 1 + M/(2r)$ in the limit $r \to \infty$. The insert shows the same functions on a log-log scale.

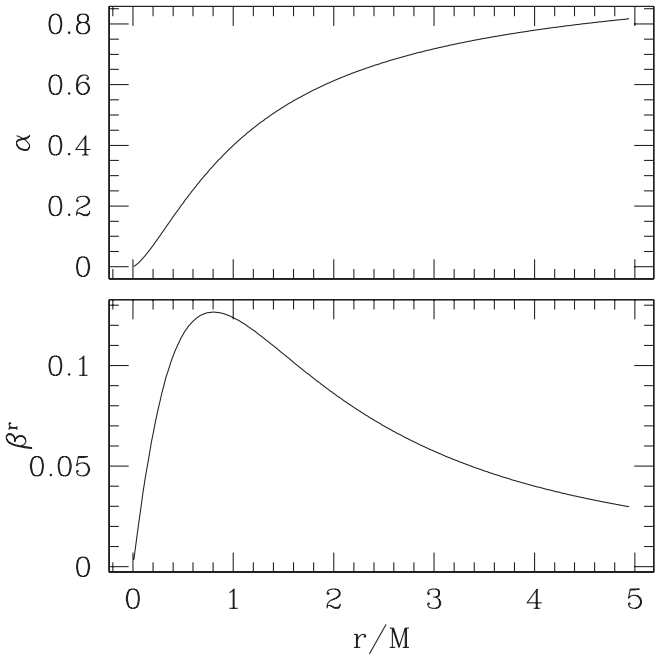

FIG. 2. The lapse α (top panel) and the shift β^r (bottom panel) as a function of isotropic radius r (Compare Fig. 5 in HHBGSO).

and the isotropic shift

$$\beta^r = \frac{dr}{dR}\beta^R = \frac{r}{R}\frac{1}{f}\frac{Cf}{R^2} = \frac{3\sqrt{3}M^2}{4}\frac{r}{R^3} \qquad (15)$$

may also be plotted vs the isotropic coordinate r (see Fig. 2) by expressing all quantities parametrically in terms of R (compare Fig. 5 in HHBGSO).

As demonstrated in HHBGSO, this solution for the conformal factor ψ, the lapse α, and the shift β^r is time independent when evolved with the slicing condition (2) for the lapse α and a $\tilde{\Gamma}$-freezing condition for the shift β^i, which, in this case, leaves the shift constant (see HHBGSO for details). Under these conditions this solution represents the asymptotic state of a moving-puncture evolution. This solution therefore provides a very useful test for moving-puncture codes: when adopted as initial data, any deviation from these initial data during the course of the evolution represents a numerical artifact and hence a measure of the numerical error. We believe that the analytic form of this solution presented in this brief report will significantly simplify the implementation and evaluation of such code tests.

This work was supported in part by NSF Grant No. PHY-0456917 and No. PHY-0456944 to Bowdoin College.

[1] F. Pretorius, Phys. Rev. Lett. **95**, 121101 (2005).
[2] M. Campanelli, C. O. Lousto, P. Marronetti, and Y. Zlochower, Phys. Rev. Lett. **96**, 111101 (2006).
[3] J. G. Baker, J. Centrella, D. I. Choi, M. Koppitz, and J. van Meter, Phys. Rev. Lett. **96**, 111102 (2006).
[4] F. Herrmann, D. Shoemaker, and P. Laguna, gr-qc/0601026.
[5] U. Sperhake, gr-qc/0606079.
[6] M. A. Scheel, H. P. Pfeiffer, L. Lindblom, L. E. Kidder, O. Rinne, and S. A. Teukolksy, Phys. Rev. D **74**, 104006 (2006).
[7] B. Brügmann, J. A. González, M. Hannam, S. Husa, U. Sperhake, and W. Tichy, gr-qc/0610128.
[8] D. Pollney, in Proceedings of New Frontiers in Numerical Relativity, Golm, 2006 (unpublished).
[9] H. Friedrich, Commun. Math. Phys. **100**, 525 (1985).
[10] D. Garfinkle, Phys. Rev. D **65**, 044029 (2002).
[11] M. Shibata and T. Nakamura, Phys. Rev. D **52**, 5428 (1995).

[12] T. W. Baumgarte and S. L. Shapiro, Phys. Rev. D **59**, 024007 (1999).
[13] S. Brandt and B. Brügmann, Phys. Rev. Lett. **78**, 3606 (1997).
[14] B. Brügmann, Int. J. Mod. Phys. D **8**, 85 (1999).
[15] M. Alcubierre, W. Benger, B. Brügmann, G. Lanfermann, L. Nerger, E. Seidel, and R. Takahashi, Phys. Rev. Lett. **87**, 271103 (2001).
[16] M. Hannam, S. Husa, D. Pollney, B. Brügmann, and N. Ó Murchadha, gr-qc/0606099.
[17] M. Hannam, S. Husa, B. Brügmann, J. A. González, U. Sperhake, and N. Ó. Murchadha, gr-qc/0612097.
[18] C. Bona, J. Massó, E. Seidel, and J. Stela, Phys. Rev. D **56**, 3405 (1997).
[19] M. Alcubierre, B. Brügmann, P. Diener, M. Koppitz, D. Pollney, E. Seidel, and R. Takahashi, Phys. Rev. D **67**, 084023 (2003).
[20] F. Estabrook, H. Wahlquist, S. Christensen, B. DeWitt, L. Smarr, and E. Tsiang, Phys. Rev. D **7**, 2814 (1973).
[21] W. Fulton, *Algebraic Topology* (Springer Verlag, New York, 1995), Chap. 20.